Australian Journal of Basic and Applied Sciences, 7(10): 608-619, 2013
ISSN 1991-8178

Structural, Optical and Thermal Characterization of ZnO Nanoparticles Doped in PEO/PVA Blend Films

[1]F.H. Abd El-kader, [2]N.A. Hakeem, [2]I.S. Elashmawi, [2]A.M. Ismail

[1]Physics department, Faculty of science, Cairo University, Giza, Egypt.
[2]Spectroscopy department, Physics division, National Research Center, Giza, Egypt.

Abstract: Solid polymer blend films based on PEO/PVA (50/50 wt/wt %) undoped and doped with different concentration of ZnO nanoparticles were prepared by using casting technique. Structural, optical and thermal studies were performed using X-ray diffraction (XRD), Fourier transform infrared (FT-IR), Ultra violet - visible spectra (UV-VIS), Scanning electron microscope (SEM), Differential scanning calorimetry (DSC) and Thermogravimetric analysis (TGA) and it's derivative (DrTG). IR absorption spectra and DSC thermograms indicate that the PEO/PVA undoped blend and doped with ZnO are immiscible. XRD and band tail energy data showed that the incorporation of nano-ZnO into the polymeric system causes decreasing the crystallinity of samples. The kinetic thermodynamic parameters such as activation energy, enthalpy, entropy and Gibb's free energy were evaluated from TG data using Coat's – Redfern relation. SEM analysis indicate that the change of the surface morphology of PEO/PVA/ZnO- nano particles system as phase segregation.

Key words: Nanocomposites; X-ray diffraction; FT-IR; Optical properties; DSC; TGA.

INTRODUCTION

Polyvinyl alcohol (PVA) polymers have attracted attention due to their variety of applications [Abdelaziz and Ghannam (2010)]. PVA is a water soluble polymer which is important from an industrial view point. Some studies reveal that the optical and thermal properties of the PVA can be controlled by doping for different applications [Devi *et al*. (2002); Zhang *et al* (2008) and Abdelaziz (2011)]. Polyethylene oxide (PEO) is the most interesting base material because of it is high chemical and thermal stability [Kumar *et al*. (2011)]. PEO is semicrystalline polymer, possessing both amorphous and crystalline phases at room temperature.

Polymer blending is one of the most important contemporary ways for the development of new polymeric materials and it is a useful technique for designing materials with a wide variety of properties [Pielichowski and Hamerton (2000)]. Polymer nanocomposites have attracted a great deal of attention in recent years due to their exceptional properties [Fragiadakis *et al*. (2005) and Momen *et al*. (2011)]. ZnO is an odd material with novel applications due to it's proper optical, electrical and thermal properties. Nano-ZnO is one of the multifunctional inorganic nanoparticles has drawn increasing attention in recent years due to it's many significant properties such as chemical stability, high catalysis activity and intensive ultraviolet and infrared absorption [Elashmawi *et al*. (2010)]. In particular, the introducing of nano-ZnO into polymeric matrix can enhance both mechanical and optical properties of the polymers due to a strong interfacial interaction between the organic polymer and the inorganic nanoparticles [Lee *et al*. (2008)]. Composites based on such nanoparticles can be widely utilised in coating, rubbers, plastics, sealants, fibers and other application. J. Lee *et al* [Lee *et al*. (2008)] described the development of PEO/PVA/nano-ZnO film, then evaluated and optimized the effect of ZnO additive on some physical properties of the polyblend polymer.

The main purpose of this work was to achieve a deeper insight into the fundamental physical properties of PEO/PVA blend films doped with different concentration of ZnO nanoparticles. A systematic investigation on miscibility, thermal stability, structure, morphology and band tail property relationship of such nano- ZnO polyblend system are discussed using different tools and techniques.

MATERIALS AND METHODS

2.1. Materials:

Poly ethylene oxide (ACROS, New Jersey, USA) with M.W. ≈ 900.000 and Poly vinyl alcohol (MP Biomedicals, Inc, France) with M.W. ≈ 15.000 were used as a basic polymeric composite materials. Nano-powder of ZnO with a mean particles size <100 nm was supplied by SIGMA-ALDRICH, USA. All chemicals were used as received without any purification.

Corresponding Author: F.H. Abd El-kader, Physics department, Faculty of science, Cairo University, Giza, Egypt.

2.2. Preparation Method:

Equal quantity of PEO and PVA (50/50 wt/wt %) was dissolved in distilled water separately and then the polymer blend solution was stirred continuously until a homogenous viscous liquid was formed. ZnO nanoparticles were also dissolved in distilled water. The resulting solution of ZnO nanoparticles was added drop by drop to the polymer solution with mass fraction 0.5, 1.0, 2.5, 5.0 and 10 %wt. The resulting solution was cast onto plastic Petri dishes and kept in a dry atmosphere at 70˚C about 48 hrs. After drying, the films were peeled from Petri dishes and kept in vacuum desiccators until uses.

2.3. Measurement Techniques:

X-ray diffractions were performed using Diano Corporation-USA equipped with Cu-Kα radiation (λ= 0.1540 nm, the tube operated at 30kV, Bragg's angle (2θ) in the range (5-60°). FT-IR measurements were performed using JASCO, FT/IR-6100 in the spectral range of 4000-400 cm^{-1}. Ultraviolet-visible absorption spectra were measured in the wave length region of 200-1000 nm using V-570 UV-VIS-NIR (JASCO, Japan) spectrophotometer. Scanning electron micrograph was performed using SEM (JEOL-JSM 6100), operating at 30KV as an accelerating voltage. Differential scanning calorimetry of the prepared samples were carried out using (DSC-50, Shimadzu, Japan) with measuring temperature range from room temperature to 400°C and the heating rate was 10°C/min. The Thermogravimetric analysis (TGA) was used to characterize the decomposition and thermal stability of prepared samples by A Perkin-Elmer TGA-7. The loss of mass was recorded during heating from ambient temperature up to 460 °C with rate of 10°C/min.

RESULTS AND DISCUSSION

3.1. X-ray Diffraction (XRD):

XRD analysis is very useful in knowing the structure of the polymeric materials. XRD patterns enable one to find out whether a material is crystalline or amorphous.

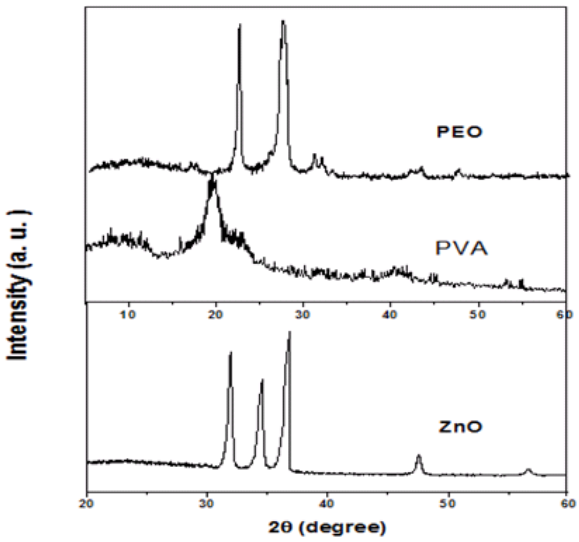

Fig. 1: X-ray diffraction of ZnO, PVA and PEO.

Figure 1 shows the X-ray diffraction patterns of PEO and PVA homopolymers and ZnO nanoparticles as powders at room temperature. Pure PEO has two well defined reflection peaks at 2θ values 19.1° and 23.3° [[Kumar *et al*. (2011)] and Sasikala *et al*. (2012)] while Pure PVA exhibits only a broad and shallow diffraction feature around the 2θ value of 20° [Saion and Teridi (2006); Abdelaziz *et al*. (2010) and Ahad *et al*. (2012)]. The reflection peaks of ZnO nanoparticles appeared at 2θ values 31.7°, 34.4°, 36.2°, 47.5° [Wen *et al*. (2008)].

Figure 2 represents the X-ray diffraction patterns of PEO/PVA blend films undoped and doped with different concentration of ZnO nanoparticles in the scanning range 5°≤2θ ≤60°. Spectrum (2a), for undoped blend sample shows well defined broad peaks at around 19° and 23°, which are unique to the feature of PEO. This result reflects that PEO remain as separate phases with no significant mixing. XRD patterns (2b-2f) of blend sample doped with ZnO show two peaks at 2θ= 19° and 23° , which their intensities slightly changed irregularly with increasing ZnO concentration but still lower than undoped one. Besides, the reflection peaks of ZnO at 2θ values 31.7˚ 34.4˚ and 36.2˚ begin to appear as small pe aks and their intensity increase with

increasing ZnO content≤ 5.0 wt%. However, further addition of ZnO concentration beyond 5.0 wt% the reflection peaks of ZnO disappeared and the crystalline fraction of polyblend system decreases. This revealed that there is a distortion in crystal structure of such system (see fig. 2f).

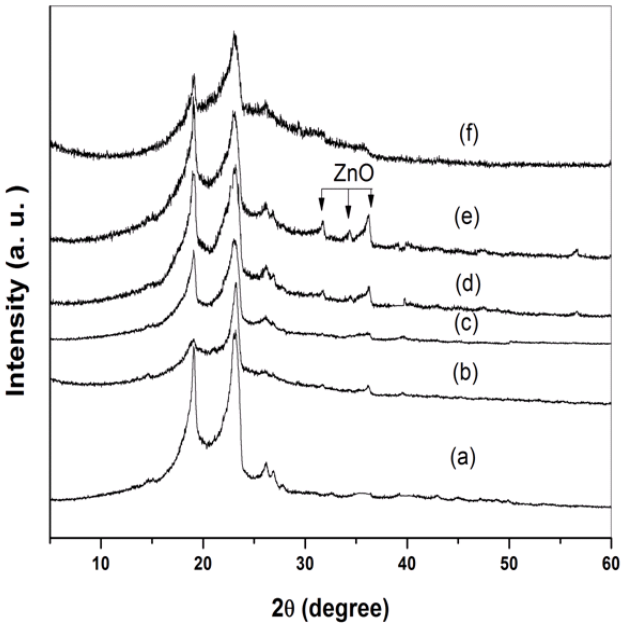

Fig. 2: X-ray diffraction of: (a) 50/50 (wt/wt. %) PEO/PVA undoped blend sample and blend sample doped with: (b) 0.5, (c) 1.0, (d) 2.5, (e) 5.0 and (f) 10 wt. % ZnO nanoparticles

Figure 3 shows the variation of the crystalline fraction of the samples as a function of ZnO concentration. Resolution of crystalline peaks, together with an integration of the scattered intensities, provides a method for the estimation of crystallinity. The degree of crystallinity (X_c), is calculated according to the Hermans-Weidinger method [Rabek (1980)].

$$X_C = \frac{A(crystalline)}{A(crystalline) + KA(amorphous)} \quad (1)$$

where A (crystalline) and A (amorphous)are areas of crystalline reflections and amorphous halo, respectively; and K is constant and can be set to unity for comparative purposes. Owing to the small amount crystalline material in most samples, these measurements may not accurately reflect the absolute degree of crystallinity, but reproducible relative values were consistently obtained. It is apparent from Figure 3 that the addition of ZnO to blend sample decreases the crystalline fraction of poly blend sample. The tendency of apparently diminution of crystallinity may be a result of ZnO nanoparticles when mixed with blend sample, which suppress recrystallization of polyblend polymer chains and inhibits crystal growth.

3.2. Fourier Transform Infrared Analysis (FT-IR):

FT-IR spectroscopy is an important tool to investigate multi-component systems, because it provides information on the specific groups found in the blend composition as well as the polymer-polymer interactions.

Figure 4 depicts the FT-IR spectra of PEO and PVA homopolymers and their blend sample of 50/50 (wt/wt %) PEO/PVA in the range 4000-400 cm^{-1}. The IR spectra of both PVA and PEO homopolymers are seem to be consistent with that previously reported [Mishra and Rao (1999); Ramesh *et al*. (2008); Shehap (2008) and Kumar *et al*. (2011);]. The most important bands feature of these samples below 2000 cm^{-1} appear to be C=O stretching vibration at 1730 cm^{-1} and 1567 cm^{-1} , O-H bending vibration at 1328 cm^{-1} and C-O-C stretching vibration around 1100 cm^{-1}. The vibrational bands appeared at 2884 and 3344 cm^{-1} correspond to υ(CH) and υ(OH), respectively. Whereas υ(COC) stretching is present only in the spectrum of PEO but υ(OH) and υ(C=O) are present only in the spectrum of PVA [Mishra and Rao (1999)]. In general, the blend comprising the two compounds shows spectrum characteristic of both, but the vibrational bands characterizing each polymer are predominate.

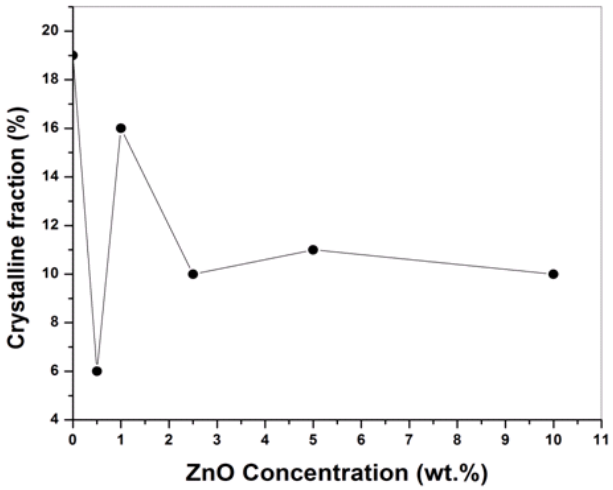

Fig. 3: Variation in crystalline fraction for 50/50 (wt/wt. %) PEO/PVA as a function of ZnO concentration.

In case of blend sample spectrum, the intensities of the most absorption bands such as υ(OH), υ(CH) and υ(COC) stretching vibrations are changed irregularly compared to their values in individual polymers, while their positions remain unaffected. Therefore intermolecular hydrogen bonding between PEO and PVA may not be significant at all [Mishra and Rao (1999)].

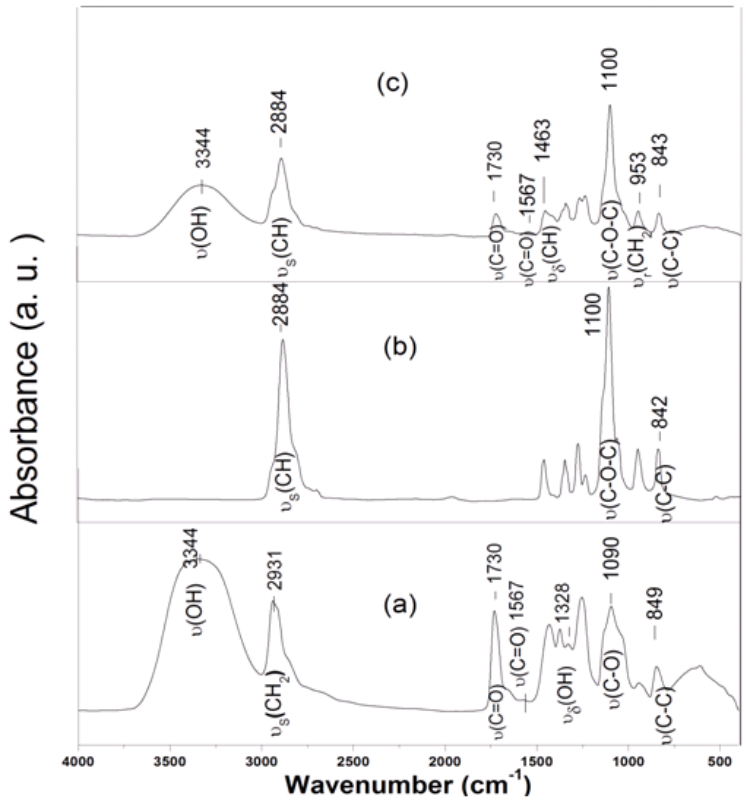

υ = Stretching S = Symmetric δ= Bending r = Rocking

Fig. 4: FT-IR absorption spectra of (a) pure PVA, (b) pure PEO and (c) 50/50 (wt/wt. %) PEO/PVA blend sample.

Figure 5 shows IR spectra for PEO/PVA blend films undoped and doped with 0.5, 1.0, 2.5, 5.0 and 10 wt. % of ZnO nanoparticles. From Figure 5 it can be seen that there is an increase in the absorption intensity of bands at 1730, 1567, 1463, 953 and 843 cm^{-1} with increasing the concentration of ZnO nanoparticles. In addition, the broadness of vibrational bands υ(OH), υ(CH) and υ(C-O-C) increase with increasing ZnO content

in blend sample. However, the absorption bands appeared at ~ 600 and ~ 527 cm^{-1} are reflected the presence of nano-ZnO vibrational groups [Wang *et al*. (2009)]. These results indicate that certain interaction occurred at the interface of ZnO nanoparticles, which act as a filler, with polyblend polymer matrix.

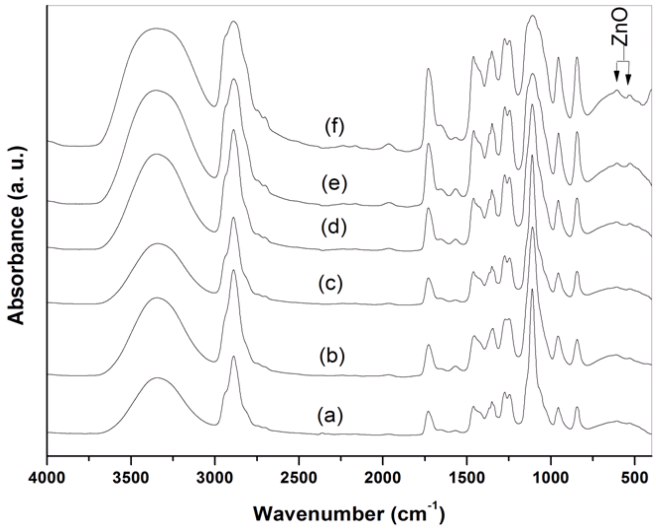

Fig. 5: FT-IR absorption spectra of: (a) (50/50wt/wt. %) PEO/PVA undoped blend sample and blend sample doped with: (b) 0.5, (c) 1.0, (d) 2.5, (e) 5.0 and (f) 10wt% of ZnO nanoparticles.

3.3. Ultraviolet-visible Spectroscopy:

UV-vis spectroscopy corresponds to electronic excitations between the energy levels related to the molecular orbital of the system. UV-vis spectra of all films are recorded at room temperature in the range of 200-800 nm as shown in Figure 6. PEO/PVA/nano-ZnO composites exhibit very small transmittance in the ultra-violet range while in visible range showed very high transmittance. Consequently these materials are considered as an optically transparent in visible region which are easily manufactured by processes that do not utilize volatile organic compounds, and whose polymer components are not environmentally hazardous. The spectrum (6a) of undoped blend sample exhibited three absorption bands, an intense band at 210 nm and a humps at 280 and 340 nm, which are related to high energy absorption. The first band was associated with the presence of some residual acetate groups of PVA and/or chromophoric groups of PEO. While the humps at 280 and 340 nm were assigned to the existence of carbonyl groups associated with ethylene unsaturation [Abdelaziz and Abdelrazek (2007)]. The bands at 280 and 340 nm may be due to $\pi \rightarrow \pi^*$ (K-band) and $n \rightarrow \pi^*$ (R - band) electronic transitions respectively. In addition, there are no absorption bands in the visible region for all samples under investigation since the films are transparent. The spectra (6b-6f) of blend samples doped with various concentrations of ZnO contain an additional band at 373 nm [Huh *et al*. (2008)], which can be assigned to Zn-O chromophoric groups. The absorption intensity of this band increases with increasing ZnO wt% content in blend sample. The absorption intensity of the bands at 280 and 340 become faint at higher concentrations≥ 2.5 ZnO wt%. In addition, only the peak position of the band at 210 nm shifted toward higher wavelengths by about 10 nm with increasing ZnO concentrations. These results support that there is an interaction between the polyblend polymer and the filler takes place.

The fundamental absorption edge is one of the most important features of the absorption spectra of crystalline and amorphous materials. The nature of optical transition involved in the blends can be determined on the basis of the dependence of absorption coefficient (α) on photon energy (hυ). The absorption coefficient (α) was calculated from the absorbance (A) [Abdelrazek *et al*. (2010)].

$$I = I_o \exp(-\alpha d) \tag{2}$$

$$\text{Hence; } \alpha = \frac{2.303}{d}\log(\frac{I_o}{I}) = \frac{2.303}{d}A \tag{3}$$

where I_o and I are the intensities of incident and transmitted radiation respectively, d is the thickness of the sample.

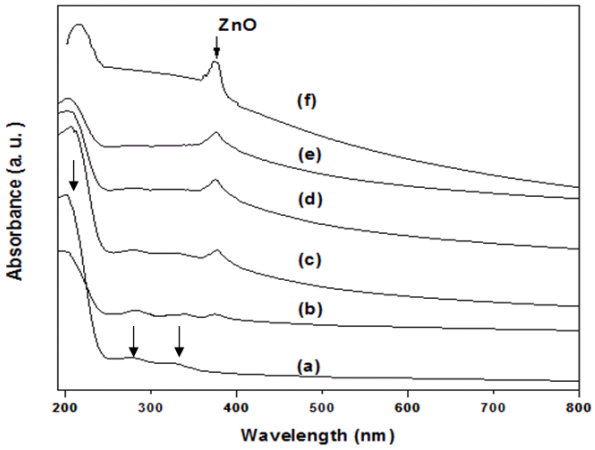

Fig. 6: UV-vis spectra of: (a) 50/50 (wt/wt. %) PEO/PVA undoped blend sample and blend sample doped with: (b) 0.5, (c) 1.0, (d) 2.5, (e) 5.0 and (f) 10 wt. % ZnO nanoparticles.

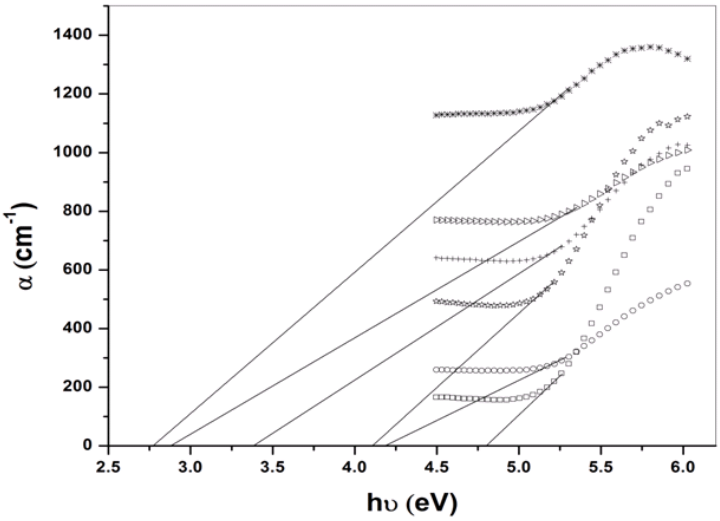

Fig. 7: Relation between absorbance coefficient (α) versus hυ for (□) 50/50 (wt/wt. %) PEO/PVA undoped blend sample and blend sample doped with; (⬯) 0.5, (☆) 1.0, (+) 2.5, (▷) 5.0 and (*) 10.0 wt% ZnO nanoparticles.

Figure 7 shows the plot of absorption coefficient with photon energy for PEO/PVA blend films undoped and doped with different concentration of ZnO. The extrapolation of the linear portion of the curves has been used to find the values of the absorption edge which are listed in Table 1. It is clear that the values of the absorption edge for doped PEO/PVA decreased as ZnO wt% increases. This may reflect the induced change in the number of available final states and/or the creation of localized states in the band gap as a result of compositional disorder [Molt and Davis (1979) and Abd El- Kader *et al*. (2010)].

The transition occurs between extended states of band and localized states of the tail of the other band and the absorption coefficient (α) is given by the Urbach relation [Urbach (1953)]:

$$\alpha(\nu) = \alpha_0 \exp\left(\frac{h\nu}{E_e}\right) \tag{4}$$

where α_0 is a constant and E_e is the width of the tail of the localized states in the band gap that associated with the amorphous nature of the materials. In general the larger the value of E_e, the greater in the structural disorder. Figure 8 shows the relation between ln α and hυ for all investigated samples. The straight lines obtained suggest that the absorption follows the quadratic relation for inter-band transitions and the Urbach rule is obeyed. The correlation factor of R^2 close to unity was choosen. The values of band tails, E_e were calculated from the slope of the straight lines and are listed in Table 1.The tail states were generated due to disorder in the system [Shehap (2008)]. It is clear that values of the band tail increases irregularly with increasing the concentration of ZnO in

blend system which confirming the increase in the disorder in such system. This result is consistent with the previous XRD data.

Table 1: The values of the absorption edge and band tail for undoped PEO/PVA and doped with different concentrations of ZnO nanoparticles.

ZnO Wt.%	Absorption edge (eV)	Band tail (eV)
0.0	4.79	0.37
0.5	4.20	096
1.0	4.10	0.75
2.5	3.37	1.51
5.0	2.86	3.12
10.0	2.70	3.01

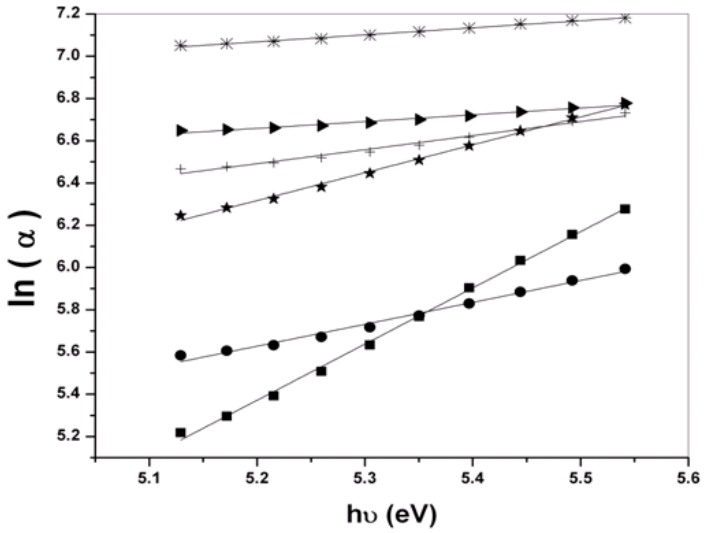

Fig. 8: Relation between ln (α) versus hυ for (■) 50/50 (wt/wt. %) PEO/PVA undoped blend sample and blend sample doped with; (●) 0.5, (★) 1.0, (+) 2.5, (►) 5.0 and (*) 10.0 wt% ZnO nanoparticles.

3.4. Scanning Electron Microscopy (SEM):

SEM is used to investigate fully the effect of ZnO nanoparticles content and to examine the dispersion of nanocomposites particles in the polyblend polymer matrix.

Figure 9 shows typical SEM images of the PEO/PVA blend without and with different concentrations of ZnO nanoparticles content. Image (a) for undoped polymer blend is found to be softer, homogenous and coherence. It is apparent that the addition of nano- ZnO particles in PEO/PVA polyblend exhibits changes in the surface morphology of such system (see images b- f). As the content of ZnO increases up to 2.5 wt% the film surface becomes roughness with some small particles (white spot) aggregates (see images b-d), which indicates segregation of ZnO in the polymeric system. Also, this result showed that there is an adhesion between the surface of ZnO nanoparticles and polyblend polymer matrix, which has been established by the organic surface modification of the ZnO nanoparticles [Matei *et al*. (2008)]. White spots on the backscattered images seem to be agglomerates of ZnO particles, which increase with increasing the concentration ZnO. Image (e) gives rise to coarse spherulitic structure, which is due to ZnO segregated into interlamellar regions of the blend. Image (f) shows smooth ganglia- like hills with some wrinkles (longitudinal shapes).

3.5. Differential Scanning Calorimetry (DSC):

DSC technique is the convenient tool to determine the physical and chemical changes such as glass transition temperatures (T_g), melting point (T_m), thermal decomposition temperature (T_d) in addition to the associated enthalpy for each process. DSC thermograms of PEO/PVA polymer blend and PEO/PVA/ZnO nanocomposites films are shown in Figure 10. The values of glass transition temperature (T_g), melting temperature (T_{m1} and T_{m2}), decomposition temperature (T_d) and heat of fusion of PVA ΔH_f (PVA) are recorded in Table 2.

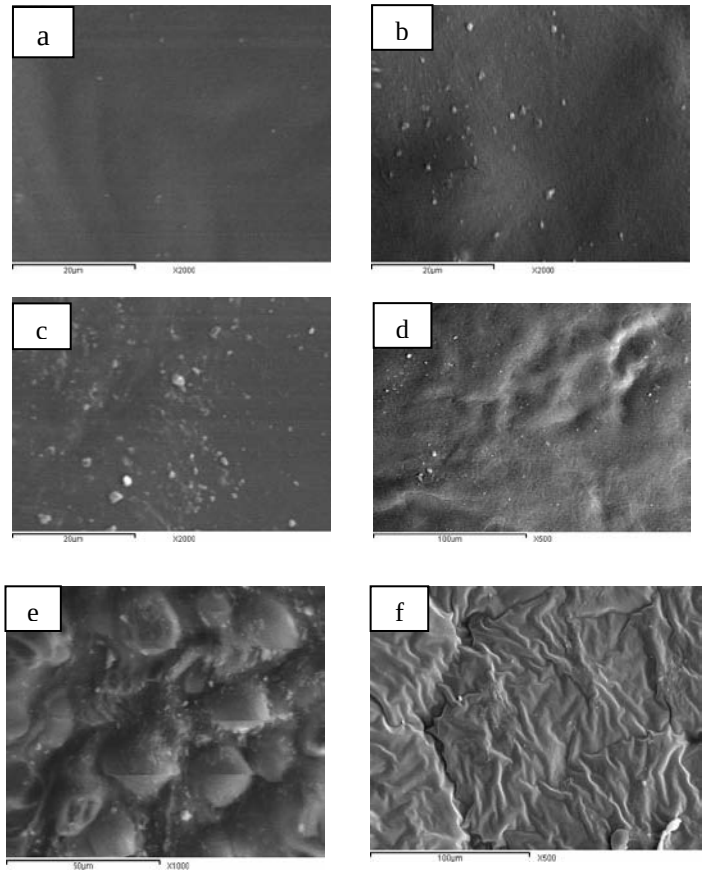

Fig. 9: SEM images of: (a) 50/50 (wt/wt. %) PEO/PVA undoped blend sample and blend sample doped with: (b) 0.5, (c) 1.0, (d) 2.5, (e) 5 and (f) 10 wt. of % ZnO nanoparticles.

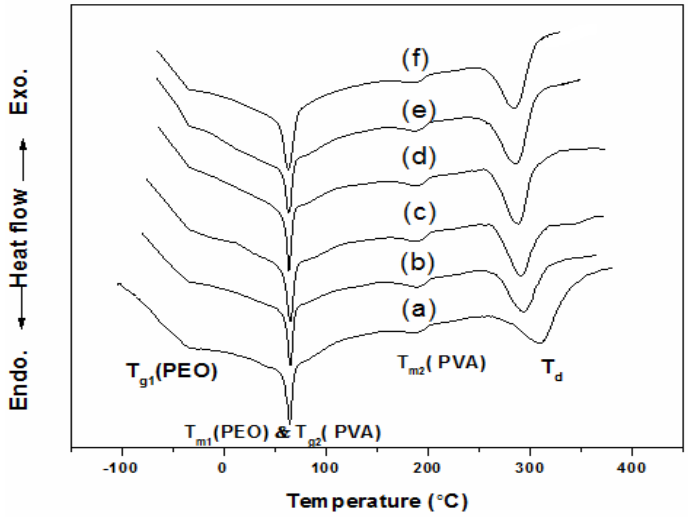

Fig. 10: DSC of: (a) 50/50 (wt/wt. %) PEO/PVA undoped blend sample and blend sample doped with: (b) 0.5, (c) 1.0, (d) 2.5, (e) 5 and (f) 10 wt. % ZnO nanoparticles.

The DSC thermograms of all samples showed four endothermic peaks.In case of undoped blend sample the first endothermic peak at about -34 ±1˚C was assigned to T_{g1} of PEO. The second endothermic peak at about 64 ±1˚C was attributed to the overlapping of T_{m1} of PEO and T_{g2} of PVA. The third endothermic peak at about 188 ±2˚C was assigned to T_{m2} of PVA. The fourth endothermic peak T_d was observed in the range between 284 up to 310˚C. It is reported previously [Lai and Liau (2004)] that the glass transition temperature of the PVA was expected to be close to 71˚C. Coincidently, it was near the melting point of PEO, 66˚C. Therefore, the glass transition peak of PVA might overlap with the melting peak of PEO in DSC thermogram and it could be difficult to observe the glass transition temperature separately. It is clear from Table 2 that the position of [T_{m1}

of PEO & T_{g2} of PVA] and T_{m2} peaks remain unaltered with increasing ZnO content in blend sample. While the position of T_d peak shifted to lower temperatures with increasing ZnO content in blend sample indicating to the decrease of thermal stability and weakening the bond strength. It is generally accepted that the presence of two separate T_g's in polymer blends provides a strong signature of immiscibility. Immiscible blends may be further described as compatible or incompatible. In the present case, the blend sample of PEO/PVA undoped and doped with ZnO nanoparticles are immiscible but still compatible.

To understand the change in the structural characteristic induced by adding ZnO nanoparticles, the crystallinity percentage (ΔC) for PVA was measured from the heat of fusion at melting for PVA by the following equation [Guirguis and Moselhey (2012)].

$$\Delta C = \frac{\Delta H_f}{\Delta H_{f(100)}} \times 100 \tag{5}$$

where ΔH_f is the heat of fusion of PVA; $\Delta H_{f(100)}$ is the heat of fusion of 100% crystallinity of pure PVA ($\Delta H_{f(100)}$= 160 Jg^{-1}) [Abdelaziz (2011)]. Since T_g of PVA is overlapped with T_m of PEO, so it is difficult to determine exactly the enthalpy associated with melting point of PEO. Thus, the calculation of the change in the crystallinity percentage for PEO with increasing ZnO concentrations is not preferable. The estimated values of the degree of crystallinity for the PVA after adding ZnO to blend film are tabulated in Table 2. It is clear from Table 2 that there is a decrease in the crystallinity percentage after the addition of different concentration of ZnO for all samples.

Table 2: The values of [T_{m1} (PEO) & T_{g2}(PVA)], T_{m2}, T_d, ΔH_f (PVA) and ΔC (PVA) for undoped PEO/PVA and doped with different concentration of ZnO nanoparticles.

ZnO Wt.%	Tm_1(PEO) & Tg_2(PVA) (°C)	T_{m2} (°C)	T_d (°C)	ΔH_f (PVA) (Jg^{-1})	ΔC (%)
0.0	64	188	310	15.52	9.70
0.5	65	189	294	14.88	9.30
1.0	65	190	292	14.56	9.10
2.5	64	189	288	14.48	9.05
5.0	63	187	285	14.40	9.00
10	63	186	284	12.01	7.50

3.6. Thermogravimetric Analysis (TGA) and it's Derivative (Dr TG):

Thermogravimetric analysis is a process in which substance is decomposed in the presence of heat which causes bonds within the molecules to be broken. The sample weight decreases slowly as the reaction begins, then decreases rapidly over a comparatively narrow temperature range and finally levels off as the reactants become spent. The shape of TGA curve depends primarily upon the kinetics parameters.

Figure 11 shows TGA and Dr TG thermograms as a function of temperature in the range from 20 °C to 460 °C for PEO/PVA blend undoped and doped with different concentrations of ZnO nanoparticles. It is clear from Figure 11 that all samples have three steps of decomposition. Table 3 represents the decomposition steps and percentage weight loss for PEO/PVA blend undoped and doped with different concentration of ZnO nanoparticles. The lower values of percentage weight loss, in the first decomposition step which include the melting point of PEO (0.90 -3.00 %) may be due to splitting or volatilization of small molecule, and/or the evaporation of moisture. The second decomposition region in TG curves which cover a wider temperature range including the melting point of PVA have a percentage weight loss (35.0- 44.0 %). The latter process in TG curves which is the main decomposition step has a more significant percentage weight loss (43.0-50.0 %).

The difference in thermal decomposition behaviour of the investigated samples can be seen more clearly from curves shown in Figure 11. DrTG curves show three temperature broad peaks T_P's corresponding to the three decomposition regions (see Table 3). It is noted that the peak temperature T_p of DrTG curves blend sample doped with various ZnO content in all regions are shifted to lower temperatures compared to undoped blend sample. This indicates that the thermal stability of blend sample decreases by mixing it with ZnO nanoparticles.

The thermodynamics activation parameters of the decomposition process were evaluated by making use of the well known Coats- Redfern equation [Coats and Redfern (1964)] for first order reaction in the form:

$$\ln\left[\frac{-\ln(1-\delta)}{T^2}\right] = -\frac{E^*}{RT} + \ln\frac{AR}{\beta E^*} \tag{6}$$

where A is constant, β is heating rate , R is the universal gas constant, δ is fraction of decomposition and E* is the activation energy. Therefore plotting $\ln\left[\frac{-\ln(1-\delta)}{T^2}\right]$ against 1/T according to equation (6) (Figure not shown for sake brevity) should give a straight line whose slope is directly proportional to the activation energy ($-\frac{E^*}{R}$). The activation entropy ΔS*, the activation enthalpy ΔH*, and the free energy (Gibbs function ΔG*) were calculating using the following equations [Yakuphanoglu *et al*. (2004)]:

$$\Delta S^* = 2.303(\log\frac{Ah}{KT})R \tag{7}$$

$$\Delta H^* = E^* - RT \tag{8}$$

$$\Delta G^* = \Delta H^* - T\Delta S^* \tag{9}$$

where k and h are Boltzmann and Planck constants respectively, T is the temperature involved in the calculation selected as the peak temperature of DrTG. The entropy ΔS* gives information about the degree of order of the system, the enthalpy ΔH* gives information about the total thermal motion and Gibbs or free energy ΔG* gives information about the stability of the system.

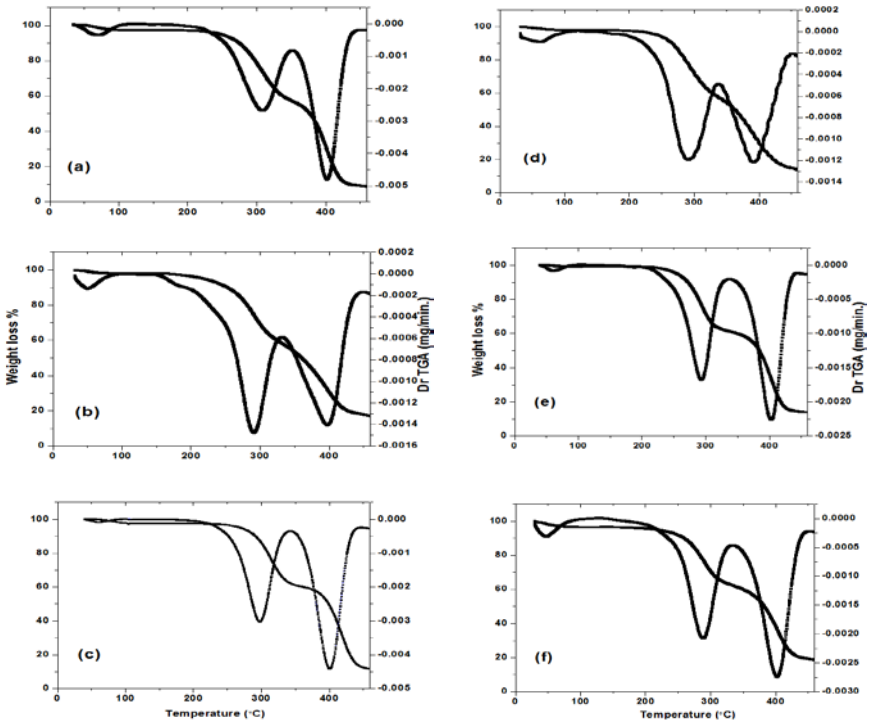

Fig. 11: TGA& Dr TGA of: (a) 50/50 (wt/wt. %) PEO/PVA undoped blend sample and blend sample doped with: (b) 0.5, (c) 1.0, (d) 2.5, (e) 5.0 and (f) 10 wt. % ZnO nanoparticles.

According the Coats- Redfern method the calculated thermodynamic parameters values are given in Table 4. It is clear that the values of E*, ΔH* and ΔS* in the second decomposition step increase with increasing ZnO concentration in blend sample. This result indicates that the addition of ZnO to PEO/PVA blend sample cause an increase of thermal motion and a decrease of the ordered of such system. However, the ΔG* values are lower than the undoped one but change irregularly with increasing ZnO concentration. In the third decomposition step the values of E*, ΔH*, ΔS* and ΔG* for doped blend samples are change irregularly with increasing ZnO concentration. Also, it is to be mentioned that the values of E*, ΔH*and ΔG* in the second decomposition step are less than those of the third decomposition step while ΔS* shows irregular trend. Thus, it can be concluded that the nature of the second decomposition region is relatively low thermal motion, more orderness and relative thermal stability of most samples with respect to the third decomposition process.

The activation energies for this nanocomposite system are small at second stages of degradation and higher at the third stages. These lower values are most likely associated with process that occurs at weak linkage of

PEO/PVA/ZnO system. By increasing the temperature, random scission of macromolecular chains predominates and the activation energy has a greater value.

Table 3: TG and D_r TG data for undoped PEO/PVA and doped with different concentration of ZnO nanoparticles.

ZnO Wt.%	Region of Decomposition	Temperature(°C)			Weight loss (%)	
		Start	End	T_p	Partial	Total
0.0	1st	38	115	69	3.00	92.0
	2nd	162	348	309	40.0	
	3rd	348	450	402	49.0	
0.5	1st	32	67	50	1.50	88.5
	2nd	132	313	290	44.0	
	3rd	314	426	397	43.0	
1.0	1st	34	97	59	2.40	88.4
	2nd	197	329	297	36.0	
	3rd	330	445	400	50.0	
2.5	1st	31	82	62	2.00	82.0
	2nd	177	326	291	37.0	
	3rd	327	433	392	43.0	
5.0	1st	40	105	60	0.90	85.9
	2nd	181	320	293	36.0	
	3rd	320	453	401	49.0	
10	1st	31	116.4	47	3.00	81.0
	2nd	156	336.2	288	35.0	
	3rd	336	455.1	401	43.0	

$T_{p:}$ Peak temperature of D_rTG

Table 4: Thermodynamic parameters for undoped PEO/PVA blend and doped with different concentrations of ZnO nanoparticles.

ZnO Wt.%	E*(kJ/mole)		ΔS*(J/K.mole)		ΔH*(kJ/mole)		ΔG* (kJ/mole)	
	2nd region	3rd region	2nd region	3rd region	2nd region	3rd region	2nd region	3rd region
0.0	101	159	-87	-32	96	153	147	175
0.5	122	139	-46	-49	117	133	142	166
1.0	122	164	-37	-15	117	158	138	168
2.5	125	142	-35	-47	120	136	140	167
5.0	130	162	-26	-20	125	156	140	170
10	132	166	-18	-14	127	160	137	170

4. Conclusions:

Although the blend films undoped and doped with ZnO formed were homogenous, coherent and showed neither separation into bilayers nor any precipitation; IR and DSC data reveal that they are immiscible. The presence of ZnO in PEO/PVA blend sample induce a decrease of crystallinity as indicated by XRD patterns and band tail in UV-visible range. TG and Dr TG data provide that thermal stability decrease as a result of addition of ZnO nanoparticles to polyblend system. As the content of ZnO increases in the polyblend sample, the surface morphology becames roughness with white spot and it reveals the tendency towards phase segregation in the interlameller regions of the polyblend chain.

Finally, it can be concluded that the film properties can be significantly modified by incorporation of nano-ZnO at a concentration $\leq$ 5.0 wt% in blend sample. At higher proportions of nano -ZnO resulting in agglomeration of ZnO particles and deterioration in film properties.

REFERENCES

Abdelaziz, M., E.M. Abdelrazek, 2007. Effect of dopant mixture on structural, optical and electron spin resonance properties of polyvinyl alcohol. Physica B, 390: 1-9.

Abdelaziz, M., M. M. Ghannam, 2010. Influence of titanium chloride addition on the optical and dielectric properties of PVA films. Physica B, 405: 958-964.

Abdelaziz, M., 2011. Cerium (III) doping effects on optical and thermal properties of PVA films. Physica B, 406: 1300-1307.

Abd El-Kader, F.H., S.A. Gafer, A.F. Basha, S.J. Bannon, M.A.F. Basha, 2010. Thermal and optical properties of gelatin/poly(vinyl alcohol) blends. J Appl Polym Sci., 118: 413-420.

Ahad, N., E. Saion, E. Gharibshahi, 2012. Structural, thermal, and electrical properties of PVA-sodium salicylate solid composite polymer electrolyte. Journal of Nanomaterials. Article ID 857569, 8 pages.

Coats, A.W., J.P. Redfern, 1964. Kinetic parameters from thermogravimetric data. Nature, 201: 68-69.

Devi, C.U., A.K. Sharma, V.V.R.V. Rao, 2002. Electrical and optical properties of pure and silver nitrate-doped polyvinyl alcohol films. Materials Letters, 56: 167-174.

Elashmawi, I.S., N.A. Hakeem, L.K. Marei, F.F. Hanna, 2010. Structure and performance of ZnO/PVC nanocomposites. Physica B, 405: 4163-4169.

Fragiadakis, D., P. Pissis, L. Bokobza, 2005. Glass transition and molecular dynamics in poly (dimethylsiloxane) /silica nanocomposites. Polymer, 46: 6001-6008.

Guirguis, O.W., M.T.H. Moselhey, 2012. Thermal and structural studies of poly(vinyl alcohol) and hydroxypropyl cellulose blends. Natural Science, 4: 57-67.

Huh, P., F. Yan, L. Li, M. Kim, R. Mosurkal, L.A. Samuelson, J. Kumar, 2008. Simple fabrication of zinc oxide nanostructures. J Mater Chem., 18: 637-639.

Kumar, K.K., M. Ravi, Y. Pavani, S. Bhavani, A.K. Sharma, V.V. R.N. Rao, 2011. Physica B, 406: 1706-1712.

Lai, W.C., W.B. Liau, 2004. Study of the Miscibility and Crystallization Behavior of Poly(ethylene oxide)/Poly(vinyl alcohol) Blends. J Appl Polym Sci., 92: 1562-1568.

Lee, J., D. Bhattacharyya, A.J. Easteal, J.B. Metson, 2008. Properties of nano-ZnO/poly(vinyl alcohol)/poly(ethylene oxide) composite thin films. Curr. Appl. Phys., 8: 42-47.

Matei, A., I. Cernica, O. Cadar, C. Roman, V. Schiopu, 2008. Synthesis and characterization of ZnO-polymer nanocomposites. Int J Mater, 1: 767-770.

Mishra, R., K.J. Rao, 1999. On the formation of poly(ethyleneoxide) - poly(vinylalcohol) blends. Eur Polym J., 35: 1883-1894.

Molt, N.F., E.A. Davis, 1979. Electronic Processes in Nancrystalline materials, 2nd ed.; Oxford University Press : Oxford, P273.

Momen, G., M. Farzaneh, 2011. Survey of micro/nano filler use to improve silicone rubber for outdoor indsulators. Rev. Adv.Mater. Sci., 27: 1-13.

Pielichowski, K., I. Hamerton, 2000. Compatible poly (vinyl chloride)/chlorinated polyurethane blends: thermal characteristics. Eur Polym J., 36: 171-181.

Rabek, J.F., 1980. Experimental Methods in Polymer Chemistry, John Wiley & Sons, New York, pp: 507-508.

Ramesh, S., T.F. Yuen, C.J. Shen, 2008. Conductivity and FTIR studies on PEO–LiX [X: $CF_3SO_3^-$, SO_4^{2-}]. Spectrochimica Acta Part A, 69: 670-675.

Saion, E., M.A.M. Teridi, 2006. Effect of radiation on conductivity of solid PVA–KOH–PC composite polymer electrolytes, Ionics, 12: 53-56.

Sasikala, U., P.N. Kumar, V.V.R.N. Rao, A.K. Sharma, 2012. Structural, electrical and parametric studies of a PEO based polymer electrolyte for battery applications. International Journal Of Engineering Science& Advanced Technology, 2: 722-730.

Shehap, A.M., 2008. Thermal and spectroscopic studies of polyvinyl alcohol/sodium carboxy methyl cellulose blends. Egypt. J. Solids, 31: 75-91.

Urbach, F., 1953. The long-wavelength edge of photographic sensitivity and electronic absorption of solids Phys. Rev., 92: 1324-1326.

Wang, Y., X. Fan, J. Sun, 2009. Hydrothermal synthesis of phosphate-mediated ZnO nanosheets. Materials Letters, 63: 350-352.

Wen, B., Y. Huang, J.J. Boland, 2008. Controllable growth of ZnO nanostructures by a simple solvothermal process. J Phys Chem C, 112: 106-111.

Yakuphanoglu, F., A.O. Gorgulu, A. Cukurovali, 2004. An organic semiconductor and conduction mechanism: N-[5-methyl-1,3,4-tiyodiazole-2-yl] itiyocarbamate compound. Physica B, 353: 223-229.

Zhang, L.Z., Y.Y. Wang, C.L. Wang, H. Xiang, 2008. Synthesis and characterization of a PVA/LiCl blend membrane for air dehumidification, Journal of Membrane Science, 308: 198-206.